First-Principles Investigations of Solid Iron at High Pressure and Implications for the Earth's Inner Core

Lars Stixrude and Evgeny Wasserman[1]

School of Earth and Atmospheric Sciences, Georgia Institute of Technology

Ronald E. Cohen

Geophysical Laboratory and Center for High Pressure Research, Carnegie Institution of Washington

Density functional theory is used to investigate the equation of state, phase stability, magnetism, elasticity, and high temperature properties of iron. The equations of density functional theory are solved with the state-of-the-art linearized augmented plane wave (LAPW) method with gradient-corrected exchange-correlation functionals. A parametric tight-binding Hamiltonian, which is fit to the results of the elaborate LAPW calculations, is used to investigate elasticity and high temperature properties, the latter in the cell model approximation. The results of these calculations show that (1) the bcc phase of iron is mechanically unstable above 150 GPa and is unlikely to exist in the inner core (2) the anisotropy of hcp iron is similar in its magnitude and symmetry to that of the inner core, indicating that this is the stable phase of iron in this region and that the inner core is either very strongly textured, or that it consists of a single crystal, and (3) iron is significantly denser than the inner core, indicating the presence of a few weight percent light alloying elements in the solid inner core.

INTRODUCTION

The inner core is a relatively small portion of the Earth's interior, with a mass comparable to the Earth's moon. Despite its small size, it has been the subject of increasing attention over the past decade. The inner core is now known to be anisotropic [*Morelli et al.*, 1986; *Woodhouse et al.*, 1986; *Tromp*, 1993], a surprising and unpredicted observation which reveals the structure of this most remote region of the Earth's interior in unprecedented detail and promises to shed new light on the origin and evolution of the core. With this discovery come new questions relating to the origin of the anisotropy, which is still unknown, the dynamics of the inner core [*Jeanloz and Wenk*, 1986; *Song and Richards*, 1996], its growth, and its interaction with the magnetic field [*Karato*, 1993].

The effect of the inner core on the magnetic field has also received new attention. Recent numerical models have shown that the inner core can have a major effect on the typical length scale of lateral variability in the field, its time variability and on its reversal frequency [*Hollerbach and Jones*, 1993]. Conversely, the magnetic field may exert torques on the inner core which cause it to rotate faster than the mantle [*Glatzmaier and Roberts*, 1995].

These new results in seismology and geomagnetism,

[1]Now at Battelle, Pacific Northwest National Laboratory, Richland, Washington

Properties of Earth and Planetary Materials
at High Pressure and Temperature
Geophysical Monograph 101

as well as long-standing questions of the composition and temperature of the inner core, focus our attention on the physics of its most abundant constituent at the extreme pressures and temperature that prevail. The fact that the pressures and temperature exceed those that are readily accessed in the laboratory means that our understanding of the physics of iron in the core is still limited. For example, the relative stability of the different phases of iron at inner core conditions, and therefore the crystalline structure of the inner core, is unknown. The elastic properties of iron are unknown at high pressure, limiting our ability to interpret seismological observations of the anisotropic, or even isotropic, structure of the inner core. The electromagnetic properties of iron such as the conductivity, or magnetic susceptibility, that govern the influence of the inner core on the field, are unknown beyond zero pressure.

First principles theory is an ideal complement to experimental approaches in this context. First principles approaches, such as density functional theory (DFT) solve the fundamental quantum mechanical equations that govern the behavior of matter with a minimum of approximations. They are completely independent of experiment, and yet are now capable of reproducing many experimental measurements. There is no difficulty in applying these methods at high pressure - calculations at high pressure are in fact marginally faster, in terms of computational load, primarily because the charge density tends to become more uniform under compression. Finally, these methods permit access to the fundamental physical mechanisms that underly bulk behavior.

We review here the contributions of the density functional theory to our understanding of iron at high pressure and of the inner core. We begin with an overview of computational methods, including the state-of-the-art linearized augmented plane wave (LAPW) method and the parametric tight binding model that is derived from the LAPW calculations [*Cohen et al.*, 1994a]. We also discuss methods that have been developed to treat the effect of temperature on the properties of iron. We then discuss applications of the LAPW method to perfect lattices of the observed phases of iron: body-centered cubic (bcc), face-centered cubic (fcc), and hexagonal close-packed (hcp), including their relative stability and their equations of state. The LAPW calculations of the bcc phase also illustrate the effect of pressure on the magnetism of iron. Predictions of the elastic constants of fcc and hcp phases allow us to determine the anisotropy in elastic wave velocities in iron and to compare with the anisotropy of the inner core. Finally, the cell model is used to determine the equation of state of iron up to core temperatures. The implications of these results for the crystalline structure of the inner core, the origin and nature of its anisotropy, its magnetic state, its composition, and temperature are discussed.

COMPUTATIONAL METHODS

Band Structure and Total Energy

All the computational methods discussed here are ultimately based on density functional theory [*Hohenberg and Kohn*, 1964; *Kohn and Sham*, 1965]. The essence of this theory is the proof that the ground state properties of a material, including its ground state total energy

$$E = T + U\left[\rho(\vec{r})\right] + E_{xc}\left[\rho(\vec{r})\right] \qquad (1)$$

are a unique functional of the charge density $\rho(\vec{r})$. T is the kinetic energy of a system of non-interacting electrons with the same charge density as the interacting system, U is the electrostatic (Coulomb) energy, including the electrostatic interaction between the nuclei, and E_{xc} is the exchange-correlation energy. A variational principle leads to a set of single-particle, Schrödinger-like, Kohn-Sham equations, with an effective potential given by

$$V_{KS} = V_{e-n}\left[\rho(\vec{r})\right] + V_{e-e}\left[\rho(\vec{r})\right] + V_{xc}\left[\rho(\vec{r})\right] \qquad (2)$$

where the first two terms are Coulomb potentials due to the nuclei and the other electrons, and the last is the exchange-correlation potential. The power of density functional theory is that it allows one to calculate, in principle, the exact many-body total energy of a system from a set of single-particle equations. In practice, this is not possible because the exact exchange-correlation functional E_{xc} is unknown. Fortunately, simple approximations to this potential have been very successful. The success of the local density approximation (LDA), which replaces V_{xc} at every point in the crystal by the accurately known exchange-correlation potential for a homogeneous electron gas of the same local charge density, can be understood in terms of the satisfaction of exact sum rules for the exchange-correlation hole [*Gunnarson and Lundqvist*, 1976]. The LDA has been shown to yield excellent agreement with experiment for a wide variety of insulators, metals, and semiconductors, but fails to predict the correct ground state for iron. More recently proposed functionals, such as the Generalized Gradient Approximation (GGA) [*Perdew and Wang*, 1992], which uses information about local charge density gradients as well as the local density, yield much improved results for 3d transition metals [*Bagno et al.*, 1989; *Leung et al.*, 1992].

The solution to the Kohn-Sham equations for the single-particle (quasi-electronic) eigenvalues, $\epsilon(\vec{k})$, and

eigenvectors, $\Psi(\vec{k})$, where $\vec{k}$ is a vector in reciprocal space, is that of the set of coupled generalized eigenvalue equations (units such that $\hbar^2/2m$=1)

$$H_{ij}\Psi_j = \epsilon O_{ij}\Psi_j \quad (3)$$

$$H_{ij}(\vec{k}) = \int \Psi_i^* \left(-\nabla^2 + V_{KS}\right) \Psi_j d\vec{r} \quad (4)$$

$$O_{ij}(\vec{k}) = \int \Psi_i^* \Psi_j d\vec{r} \quad (5)$$

where **H** and **O** are the Hamiltonian and overlap matrices, respectively. Because the Kohn-Sham potential is a functional of ρ, the eigenvalue equations must be solved self-consistently with the definition of the charge density in terms of the wavefunctions. First principles methods solve Equations (3-5) by expanding the wavefunctions and the potential in a complete and computationally convenient basis, $\Psi_i = c_{ij}\phi_j$.

The choice of basis functions in the LAPW method [*Wei and Krakauer*, 1985] explicitly treats the first-order partitioning of space into near-nucleus regions, where the charge density and its spatial variability are large, and interstitial regions, where the charge density varies more slowly. A dual-basis set is constructed, consisting of plane-waves in the interstitial regions that are matched continuously to more rapidly varying functions inside spheres centered about each nucleus. The advantages inherent in the LAPW method - no approximations to the shape of the charge density, potential, or to the nature of bonding - are expected to be particularly important in high pressure studies where qualitative changes in the nature of the electronic structure, such as insulator-metal transitions, changes in valence state, and coordination, may be induced by large compressions. The method is equally applicable to essentially all the elements of the periodic table, to metals, insulators, semi-conductors, and magnetic materials. The only essential limitations of the method are those inherent in the LDA or GGA approximations.

There are two major differences between tight binding methods, originally formulated by *Slater and Koster* [1954], and the first principles approaches discussed so far. First, the basis functions are chosen to be centered on the nuclei. For basis functions $\phi_{i\alpha}(\vec{r} - \vec{R}_i)$, where α labels the type of orbital (e.g., s, p, d, ...), and i labels the atom, the Hamiltonian matrix then consists of elements

$$H_{i\alpha j\beta}(\vec{k}) =$$

$$\sum_{l=0}^{\infty} \exp(i\vec{k}\cdot\vec{R}_{ij}(l)) S_{\alpha\beta}(\hat{R}_{ij}(l)) h_{\alpha\beta}(R_{ij}i(l)) \quad (6)$$

$$O_{i\alpha j\beta}(\vec{k}) =$$

$$\sum_{l=0}^{\infty} \exp(i\vec{k}\cdot\vec{R}_{ij}(l)) S_{\alpha\beta}(\hat{R}_{ij}(l)) o_{\alpha\beta}(R_{ij}i(l)) \quad (7)$$

where $R_{ij}(l)$ is the distance between the i-th atom in the reference unit cell (labeled $l = 0$) and the j-th atom in the l-th unit cell, the $S_{\alpha\beta}$ are functions of direction only and, in the two-center approximation, the $h_{\alpha\beta}$ and $o_{\alpha\beta}$ are functions only of internuclear distance. Indices i and j run over all atoms in the unit cell, and l runs over all unit cells. Under the assumption that the basis set consists of functions with the symmetry of s, p, d, ... atomic orbitals, the functions $S_{\alpha\beta}$ can be written in terms of spherical harmonics. The distance dependent functions, $h_{\alpha\beta}$ and $o_{\alpha\beta}$, are taken to be parametric functions of distance, with parameters chosen such that first principles results are reproduced. In this way, all explicit reference to the wavefunctions or charge density is eliminated. This simplifies the calculations tremendously, but renders the calculation non-self-consistent.

The non self-consistency of the tight binding approach has a very important consequence which has not been widely recognized [*Cohen et al.*, 1994a]. In general, the total energy can be written

$$E = \sum_i \int \epsilon_i(\vec{k}) d\vec{k} + F[\rho(\vec{r})] \quad (8)$$

where the first term is a sum over the self-consistent eigenvalues, and the second term, a functional of the charge density, contains all non-band structure contributions to the energy. The band structure now contains an arbitrary zero which must be fixed in order to calculate the total energy. The arbitrariness of the energy zero in the tight binding method can be exploited to recast the total energy as

$$E = \sum_i \int \epsilon_i'(\vec{k}) d\vec{k} \quad (9)$$

where the new eigenvalues are shifted in energy such that $\epsilon_i' = \epsilon_i - F[\rho(\vec{r})]$. With this formulation, the total energy is given simply as a sum over the bands, eliminating the need for pair potential repulsive terms which are often included in other treatments. The parameters of the tight binding model are determined by fitting to accurate LAPW band structures and total energies. This approach has been very successful in describing the properties of monatomic systems, such as iron [*Cohen et al.*, 1994b].

For a given arrangement of nuclei (crystal structure) the LAPW or tight binding total energy methods allow one to determine the total energy and charge density,

and the quasi-particle eigenvalue spectrum (electronic band structure). By examining the dependence of the total energy on perturbations to the volume V or shape of the crystal (described by the deviatoric strain tensor, ϵ'_{ij}), or to the positions of the atoms, the Helmholtz free energy as a function of V, ϵ'_{ij}, and T can in principle be deduced. Assuming that the deviatoric strain is small and that the stress is hydrostatic [*Wallace*, 1972]

$$F(V,\epsilon'_{ij},T) =$$

$$F_0(V) + F_{TH}(V,T) + \frac{1}{2}C_{ijkl}(V,T)\epsilon'_{ij}\epsilon'_{kl} \qquad (10)$$

where F_0 is the static (zero temperature) contribution, F_{TH} is due to the thermal excitation of electrons and phonons, and C_{ijkl} is the elastic constant tensor. This equation shows that the difference in Helmholtz free energy between a strained and unstrained lattice is in general related to a combination of elastic constants. We have made use of this to determine the full elastic constant tensor by applying a minimal set of high symmetry, volume conserving strains [*Mehl et al.*, 1990; *Stixrude and Cohen*, 1995a].

Thermal Properties

The temperature in the core far exceeds its Debye temperature so that the phonon spectrum is fully populated. In this limit, we can write F_{TH} in (10) as

$$F_{TH}(V,T) = F_{el}(V,T) - kT\ln Z \qquad (11)$$

where F_{el} is due to the thermal excitation of electrons and Z is the (classical) statistical mechanical partition function associated with atomic vibrations in the canonical ensemble

$$Z = \lambda^{-3N}\int \exp\left(-\beta(U(\vec{r}^{\,N}))\right) d\vec{r}^{\,N} \qquad (12)$$

where $\lambda = h/(2\pi m k_B T)^{1/2}$ is the de Broglie wavelength of the atoms, k_B is Boltzmann's constant, h is Planck's constant, $\beta = (k_B T)^{-1}$, U is the total energy, and $\vec{r}^{\,N}$ indicates integration over the Cartesian coordinates of N atoms ($N \approx 10^{23}$). Evaluation of this quantity requires an integration of a functional of the total energy over all vibrational degrees of freedom, an impossible task using a purely first principles approach.

In order to treat the vibrational degrees of freedom, we make use of a mean-field approximation known as the cell model [*Holt et al.*, 1970; *Ree and Holt*, 1973; *Cowley et al.*, 1990]. The motivation for using the cell model is that it accounts for anharmonicity and is computationally efficient, permitting precise determinations of all thermodynamic properties including free energies. Alternative methods for evaluating the vibrational partition function either ignore anharmonicity (e.g., quasi-harmonic lattice dynamics), or, as in the case of molecular dynamics, make fewer approximations, but are tens of thousands of times less efficient computationally.

The essential feature of the cell model is that the vibration of an atom is assumed to be uncorrelated with that of its neighbors, an approximation which is expected to be good at high temperature. In this limit, the partition function factorizes

$$Z_{cell} = \lambda^{-3N}\left[\int_{\Delta} \exp\left(-\beta(U(\vec{r}) - U_0)\right) d\vec{r}\right]^N, \qquad (13)$$

where the integral is now over the coordinates of a single atom within its Wigner Seitz cell Δ. Here U_0 is the potential energy of the system with all atoms on ideal lattice sites, $U(\vec{r})$ is the potential energy of the system with the wanderer atom displaced by the radius-vector $\vec{r}$ from its equilibrium position, and N is the total number of atoms in the system.

The pressure due to the thermal excitation of electrons is readily evaluated and is calculated with the same accuracy as the static pressure. This contribution is determined by performing self-consistent high temperature density functional calculations [*Mermin*, 1965; *McMahan and Ross*, 1977]. We have shown [*Wasserman et al.*, 1996] that this term is well approximated by a rigid band picture in which the band structure is assumed to be independent of temperature. We have assessed the accuracy of this assumption by comparing with fully self-consistent high temperature LAPW calculations. The temperature dependence of the band structure - which arises because the charge density, and therefore the potential change as higher lying states are populated - has a negligible effect on bulk thermodynamic properties.

RESULTS

Total Energy of Perfect Lattices

Calculations of the total energy of bcc, fcc, and hcp phases of iron over a range of volumes that span the pressure regime of the Earth's interior, show that density functional calculations are capable of describing the compression, phase stability, and magnetism of iron. They also clearly show the advantages of the GGA approximation to the exchange-correlation functional over the older LDA approximation [*Stixrude et al.*, 1994].

Both GGA and LDA correctly predict that hcp iron is the equilibrium low-temperature structure at high pressure (Figure 1). Moreover, GGA correctly predicts that

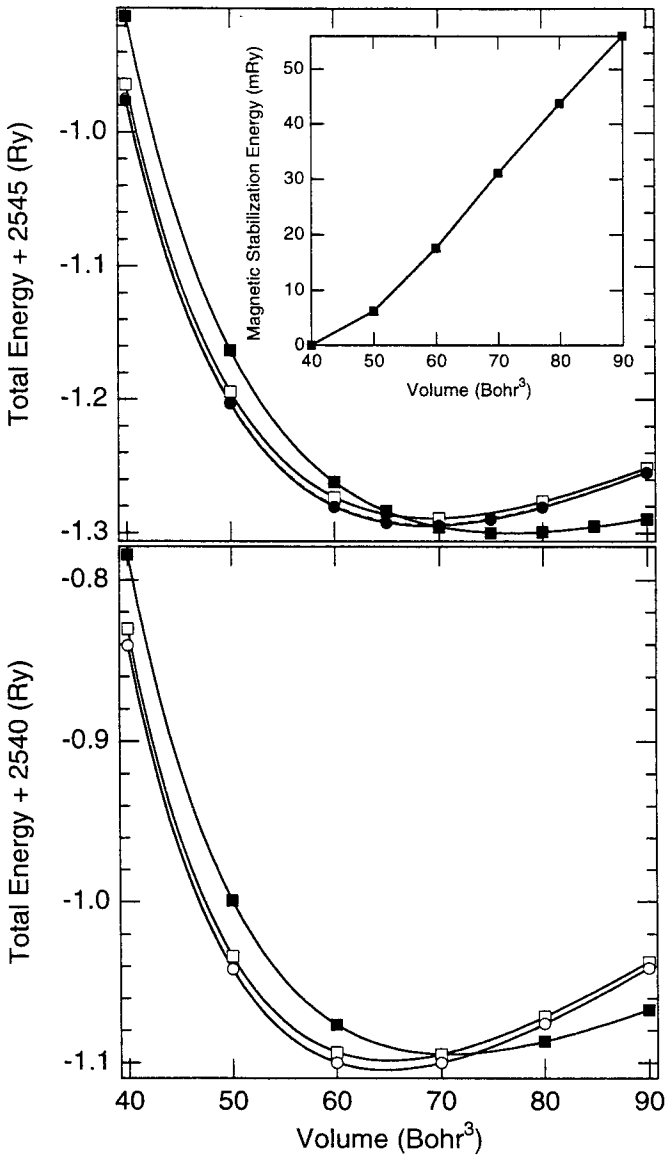

Figure 1. LAPW calculations of the total energy of iron in GGA (top) and LDA (bottom) approximations. Results for ferromagnetic bcc (filled squares), non-magnetic fcc (open squares), and hcp (circles) are shown. Results for both ideal (open circles) and minimum energy (filled circles) *c/a* ratios are shown for the hcp phase. The inset shows the magnetic stabilization energy of bcc: the difference in total energy between non-magnetic and ferromagnetic states. From *Stixrude et al.* [1994].

ferromagnetic bcc is the ground state structure, stable at zero pressure, as first shown by *Bagno et al.* [1989]. The incorporation of gradient corrections (the GGA functional) thus corrects a well known deficiency of the LDA, that it does not recover the correct ground state. We used the common tangent construction to determine the phase transition pressure from bcc to hcp predicted by the GGA calculations (Figure 2). The result, 11 GPa, is in excellent agreement with experimental observations and other density functional calculations [*Asada and Terakura*, 1992; *Söderlind et al.*, 1996]. This is an important illustration of the accuracy of density functional theory and the GGA - phase transition pressures are among the most challenging of experimental observations to reproduce theoretically because they depend on small differences between large numbers. For example, to accurately reproduce the bcc to hcp total energy difference at zero pressure requires one to calculate the total energy correctly to 8 significant figures.

In order to determine the equation of state of the three known phases of iron, we fit our total energy results to a *Birch* [1952] Eulerian finite strain expansion (Figure 3). Expansions to third order in finite strain were found to yield excellent fits to the total energies over the more than twofold compression range of our study (rms misfits were slightly less than the precision of the calculations, i.e., 0.1 mRy). The equation of state parameters determined from our GGA calculations [*Stixrude et al.*, 1994] show good agreement with the experimentally measured equation of state of bcc iron. The zero pressure volume and bulk modulus of

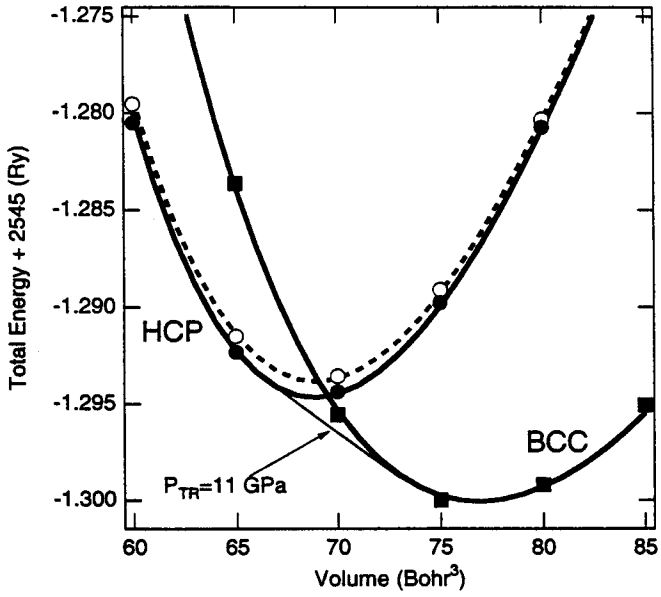

Figure 2. Detail of Figure 1 (top) showing the region of the bcc to hcp transition in the GGA approximation. Total energies of ferromagnetic bcc (closed squares), hcp with ideal *c/a* ratio (open circles and dashed line), and hcp with minimum energy *c/a* ratio (closed circles with solid line) are shown. The short thin line is the common tangent to bcc and hcp curves and represents the phase transition pressure (P_{TR}) between the two phases.

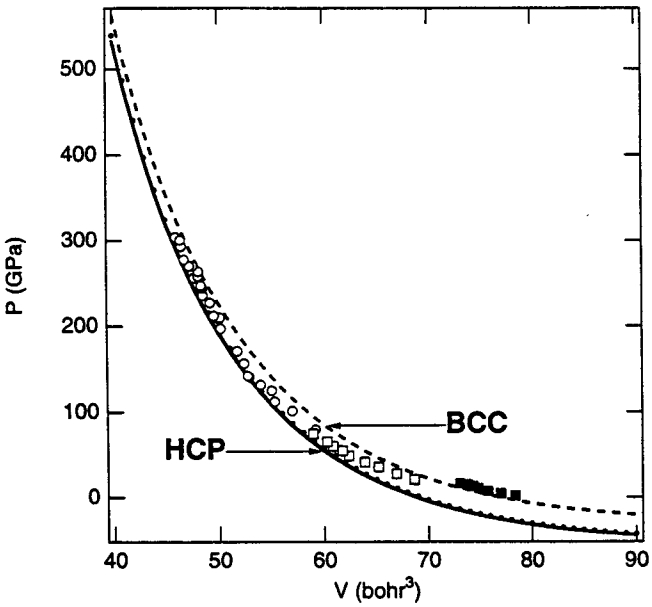

Figure 3. GGA equations of state of bcc (dashed), fcc (dotted), and hcp (solid) phases of iron compared with the experimental data of *Jephcoat et al.* [1986] (bcc, filled squares; hcp, open squares) and *Mao et al.* [1990] (hcp, open circles). From *Stixrude et al.* [1994].

the bcc phase predicted by GGA are within 3 and 10% of experiment. The agreement between GGA and the experimentally determined zero pressure properties of hcp iron is not as good. The theoretical zero pressure volume is 9% smaller than the experimental value extrapolated to zero pressure. This level of disagreement is surprising in light of the much better agreement with the zero pressure properties of the bcc phase and the performance of density functional theory in other systems, including nonmagnetic fcc 3d transition metals [*Leung et al.*, 1992]. We speculate that the discrepancy may be caused by the presence of magnetism in hcp iron at very low pressures. We have investigated only the non-magnetic state of the hcp phase as previous calculations have indicated that the ferromagnetic moment is zero for non-negative pressures [*Asada and Terakura*, 1992]. In all cases GGA agrees better with experiment than does LDA. The gradient corrections partially correct the well known tendency of local functionals to underestimate the volume.

The agreement between experiment and theory is significantly better at high pressure. At the lowest pressure at which the volume of hcp iron is actually measured, GGA and experiment differ by 6% in volume. Significantly, at the pressures of the Earth's core (136-363 GPa) GGA reproduces the experimental equation of state to within 2 %, and to within 1 % at inner core pressures (328-363 GPa). These results have been confirmed by *Sherman* [1995] also using the LAPW method and by *Söderlind et al.* [1996] using the full potential linear muffin tin orbital (LMTO) method. The agreement between different theoretical results is significant because it demonstrates the reproducibility of first principles calculations even, as in the case of *Söderlind et al.*, when different computational methods are used to solve the Kohn-Sham equations.

We use our results to address the relative stability of bcc, fcc, and hcp phases at high temperature [*Stixrude and Cohen*, 1995b]. The relative stability of these phases at core temperatures will depend on thermal contributions to their free energy. Without evaluating these thermal contributions explicitly, we find that the static total energy of the bcc structure at high pressure is so much higher than that of hcp that its stability at any temperature is highly unlikely. The total enthalpy, $H = E + PV$ of the bcc structure becomes much larger than that of hcp at high pressure. This is primarily a result of the larger volume of the bcc structure (Figure 4). The relative stability of bcc and hcp structures is governed by the difference in Gibbs free energies, G

$$\Delta G = \Delta H - T\Delta S \tag{14}$$

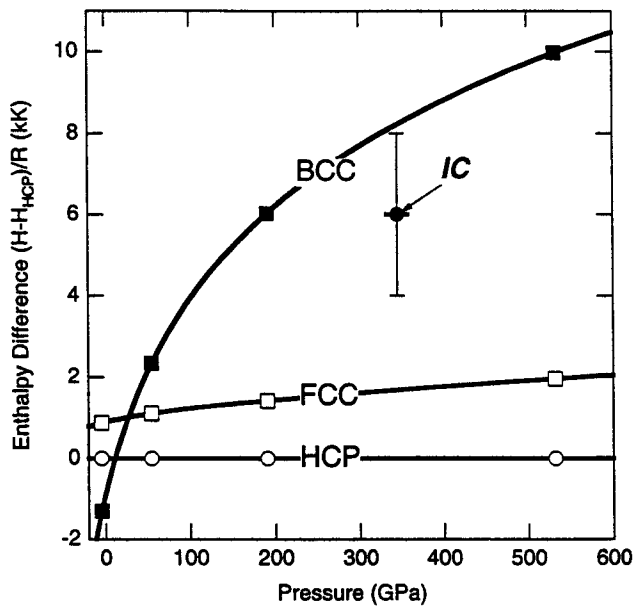

Figure 4. GGA total enthalpy of bcc (solid squares) and fcc (open squares)relative to that of hcp (open circles) as a function of pressure. The enthalpy difference is divided by the universal gas constant (R) resulting in units of temperature. Enthalpy differences are compared with the pressure range (horizontal bar) and range of estimates of the temperature (vertical error bar) of the inner core (IC). From *Stixrude and Cohen* [1995b].

where $\Delta G = G_{bcc} - G_{hcp}$. For the bcc structure to be stable with respect to the hcp structure at temperature T, we require

$$T > \Delta H/\Delta S \qquad (15)$$

If we take typical entropies of melting as an upper bound on the entropy difference, $\Delta S < R$, where R is the gas constant, then the bcc structure is stable for temperatures $T > 8000$ K at inner core pressures. This temperature exceeds even the highest estimates of the temperature in the Earth's inner core. Moreover, it exceeds the highest estimates of the melting temperature of iron at inner core pressures. The stability of the bcc structure at inner core conditions is thus highly unlikely. The energetic unfavorability of bcc at high pressure was recently confirmed by *Moroni et al.* [1996], who combined LMTO calculations with an approximate treatment of the vibrational contribution to the free energy.

Magnetism

In the crustal environment, temperature plays a crucial role in determining the magnetic state of metals and transition metal-bearing silicates and oxides. The entropy of orientational disorder of magnetic moments becomes favorable at high temperatures and leads to a vanishing net magnetic moment above the Curie temperature. However, local magnetic moments survive and are often essentially unchanged in magnitude from their values in the magnetic low temperature structure. At core pressures, a different phenomenon occurs; the local magnetic moments themselves vanish under compression.

At zero pressure our GGA calculations of the ferromagnetic state of bcc iron [*Stixrude et al.*, 1994] show that the theoretical magnetic moment is in excellent agreement with experiment (2.174 vs. 2.12 μ_B) (Figure 5). Interestingly, and despite the failure of the LDA to recover the correct ground state for iron, the magnetic moment that it predicts for (metastable) ferromagnetic bcc iron is essentially identical to that predicted by GGA at the same volume.

Our GGA and LDA calculations show that the magnetic moment of ferromagnetic bcc iron vanishes at high pressure (Figure 5). The density at which the moment approaches zero is similar to that of the inner core ($V \approx 48$ Bohr^3). The dependence of the magnetic moment on volume is quasi-linear between V=60 and 90 Bohr^3, but then begins to decrease much more rapidly at smaller volumes. These results have been confirmed by *Söderlind et al.* [1996], whose LMTO calculations show an essentially identical dependence of magnetic moment on compression.

The collapse of the magnetic moment in iron can be understood in terms of band broadening. Many

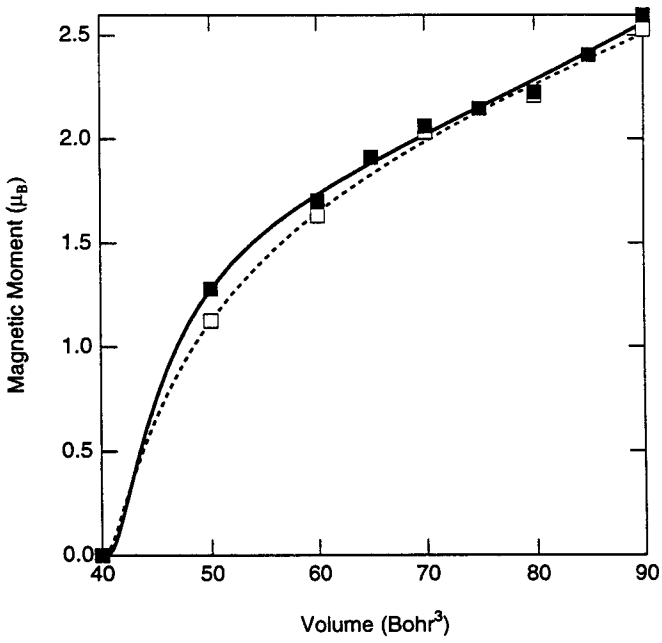

Figure 5. Magnetic moment of bcc iron in the GGA (solid squares, solid line) and LDA (open squares, dashed line) approximations in units of Bohr magnetons. From *Stixrude et al.* [1994].

transition metals are metallic because of the strong localization characteristic of d-states. These localized states produce a very narrow band with little dispersion through the Brillouin zone. However, under compression, the dispersion of these states increases because of enhanced d-d hopping, broadening the d-band and destroying their unique character. These arguments can be formalized in terms of a Stoner model [*Marcus and Moruzzi*, 1988].

Iron at densities comparable to, or slightly higher than that of the inner core, is expected to be nonmagnetic. It is worth re-emphasizing that this is a consequence of pressure, not of temperature. Pressure causes local magnetic moments to vanish. Without local moments, the concept of a Curie temperature, and the ability of high temperature to disorder moments has no significance.

Elasticity

The simplest elastic distortion of the cubic phases of iron - a stretching along one crystallographic axis - reveals a structural relationship between the bcc and fcc lattices, and the mechanical instability of the bcc phase [*Stixrude et al.*, 1994; *Stixrude and Cohen*, 1995b]. The bcc structure is recovered for c/a=1, while the fcc structure is obtained when $c/a = \sqrt{2}$. We investigated the total energy of iron as a function of the c/a ratio of this

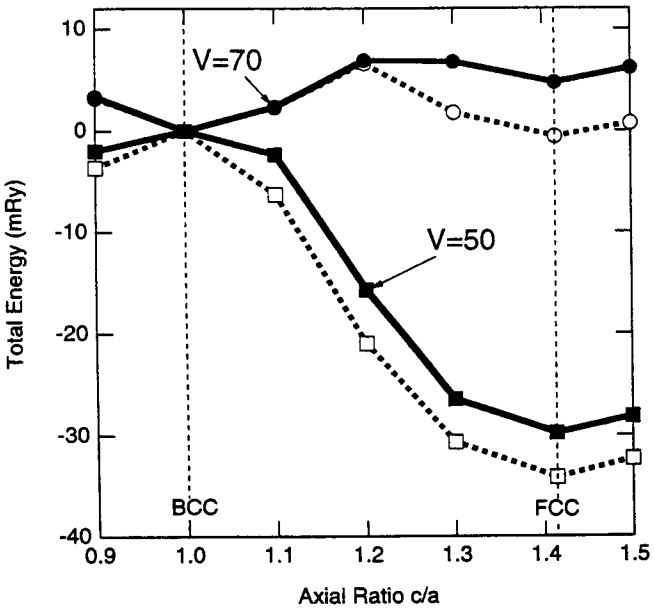

Figure 6. Total energy of iron as a function of c/a ratio. The values of c/a which correspond to the bcc (1.0) and fcc ($\sqrt{2}$) are indicated. Results at a volume of 70 Bohr^3 (near zero pressure, circles) are compared with those at 50 Bohr^3 (near 200 GPa, squares). Ferromagnetic GGA results are indicated by the filled symbols, ferromagnetic LDA results by the open symbols. From *Stixrude et al.* [1994].

tetragonal lattice with the LAPW method and using both LDA and GGA exchange-correlation functionals.

At low pressure, the total energy as a function of c/a ratio displays two local minima, one corresponding to the bcc structure and one to the fcc structure (Figure 6). This is in agreement with experimental observation. Both of these phases are known to be elastically stable at low pressure. In both theory and experiment, as the lattices are strained, their total energy rises, corresponding to an elastic restoring force. At high pressure, a completely different picture is revealed by our theoretical results. While the fcc phase is still elastically stable, the bcc phase is elastically unstable. As the bcc lattice is strained by small amounts, its energy is lowered. This means that there is no restoring force that preserves the bcc structure at high pressure. In the presence of infinitesimal thermal fluctuations, the bcc lattice will undergo a spontaneous distortion to the fcc structure. The mechanical instability of the bcc lattice was recently confirmed by *Söderlind et al.* [1996], whose LMTO calculations show mechanical instability for volumes less than approximately 55 Bohr^3, consistent with our results.

The mechanical instability of the bcc lattice can also be understood in terms of the Born stability criterion. The second derivative of the total energy with respect to c/a is proportional to the combination of elastic constants $C_S = C_{11} - C_{12}$ which must be greater than zero for a mechanically stable structure. The negative curvature exhibited by bcc above 150 GPa corresponds to a negative value of C_S and violation of the Born criterion.

There is no evidence for a stable tetragonal structure in iron at any pressure. Such a structure was proposed by *Söderlind et al.* [1996] on the basis of the apparent local minimum in total energy for $c/a < 1$ (Figure 7). It is important to recognize that this minimum is merely a saddle point and does not correspond to a mechanically stable structure. This becomes clear when one considers the orthorhombic strain energy surface. The fcc structure can be derived from the bcc structure in one of two ways: (1) by increasing the c/a ratio or (2) by decreasing c/a and b/a. By decreasing c/a below unity, a structure is generated which is intermediate between bcc and fcc. Tight-binding calculations at a series of volumes that span inner core conditions ($V = 40 - 50$ Bohr^3) confirm that the apparent local minimum is a saddle point and does not represent a mechanically stable structure.

Because the bcc phase is not only energetically unfavorable, but also mechanically unstable, it is highly unlikely to exist in the Earth's core. We investigated the elasticity of the remaining observed phases of iron, fcc

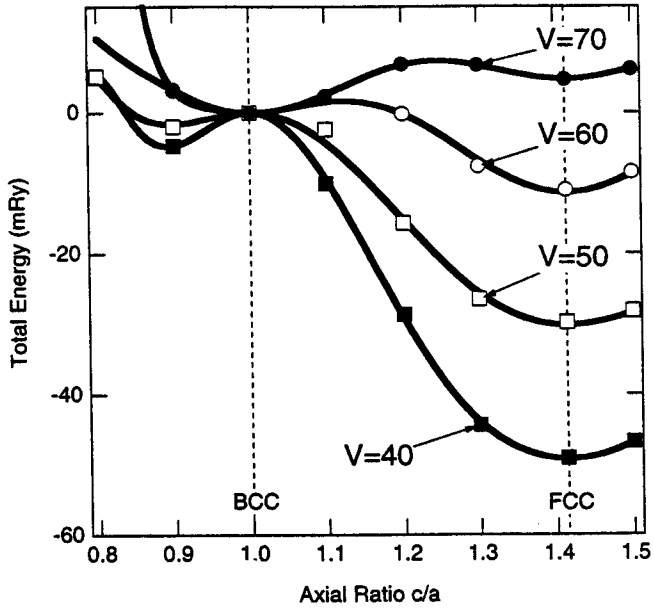

Figure 7. Total energy of iron as a function of c/a ratio in the GGA approximation. Results at four volumes are shown as indicated. The horizontal axis is extended towards smaller c/a ratios to illustrate the apparent minimum which develops near c/a=0.9 for V=50 and 60 Bohr^3.

and hcp in more detail with the tight binding method. We used this model to determine the full elastic constant tensor of both phases.

The elastic constants as a function of pressure of fcc and hcp iron are shown in Figure 8. We find that the elastic constants depend sublinearly on pressure. In the case of hcp, the diagonal elastic constants are similar in magnitude with C_{33} slightly larger than C_{11} at all pressures (by 6% at inner core densities). Similarly, $C_{66} = (C_{11} - C_{12})/2$ is slightly larger than C_{44} (by 5% at inner core densities). The differences between these pairs of elastic constants correspond to anisotropies in P- and S-wave velocities.

Our predicted fcc and hcp elastic constants are in generally good agreement with LMTO results [*Söderlind et al.*, 1996]; the RMS difference between the two sets of predictions is 70 GPa, or 6% at inner core densities. The largest difference occurs in C_{12} of hcp: while we find that C_{12} and C_{13} are similar, differing by no more than 6%, the LMTO study finds that C_{12} is more than 50% smaller than C_{13} at inner core densities. While the cause of this discrepancy is unclear, we note that experimental data on other hcp transition metals [*Brandes*, 1983] show $C_{12} \approx C_{13}$, consistent with our results. Moreover, *Söderlind et al.* performed their elastic constant calculations using the ideal, rather than the equilibrium value of c/a. We speculate that this may have biased their results.

The elastic constants completely specify elastic wave propagation in a single crystal as a function of propagation direction $\vec{n}$ and polarization direction $\vec{w}$. The wave velocities V are given by the eigenvalues of the Cristoffel equation

$$C_{ijkl} n_j w_k n_l = \rho V^2 w_i \qquad (16)$$

where ρ is the density. We find that the magnitude of the anisotropy is threefold greater in the cubic phase and threefold greater for S-waves than for P-waves: at the density of the inner core (V=48 Bohr^3) P-wave velocities vary with propagation direction by 10 and 3%, respectively in fcc and hcp, while S-wave velocities are 30 and 10% anisotropic (Figure 9). The greater anisotropy of the cubic structure, the directions of maximum and minimum velocities, and the greater anisotropy of S-waves can be understood in terms of a parameter free nearest neighbor central force model [*Born and Huang*, 1954]. The magnitude of the P-wave anisotropy in hcp is very similar to that observed seismologically in the inner core.

We may also compare the absolute values of elastic wave velocities determined theoretically with those of radial seismological models. The theoretical P- and S-wave velocities of isotropic aggregates of iron are higher

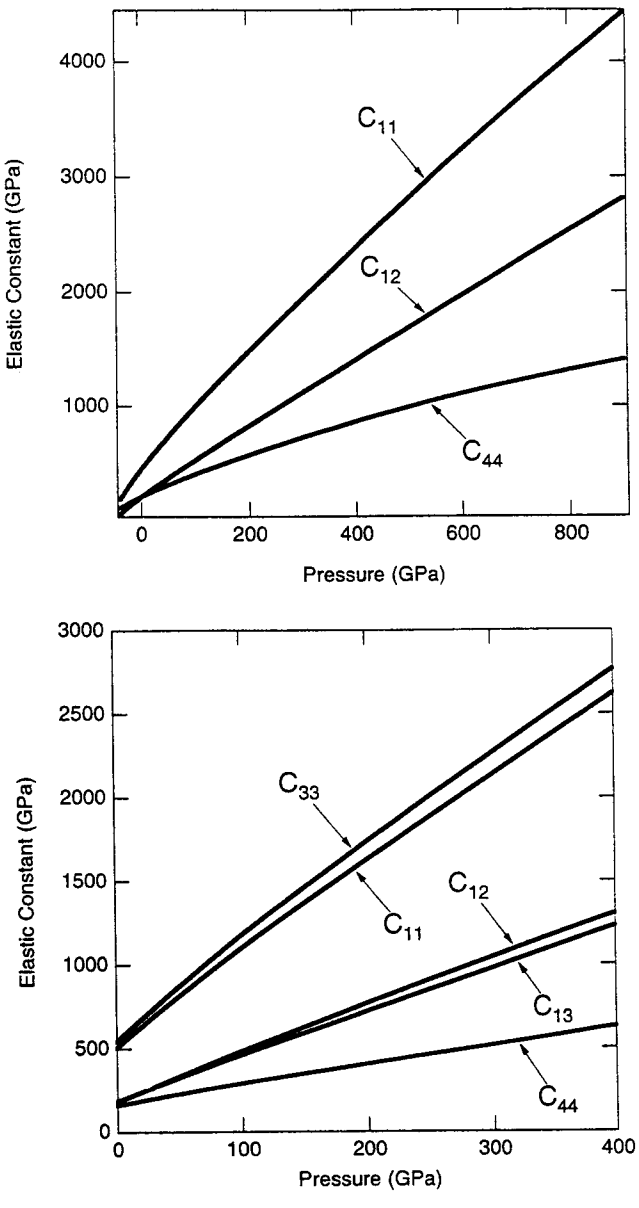

Figure 8. Elastic constants of fcc (top) and hcp (bottom) iron as a function of pressure.

than those observed for the inner core by 5 and 50%, respectively [*Stixrude and Cohen*, 1995a]. This difference is due to the difference in temperature between the static calculations and the inner core, and to the relatively low frequencies of seismic waves; our theoretical elastic constants correspond to infinite frequency values. One way to illustrate this is to compare the Poisson's ratio σ from our calculations with that of the inner core. We find that $\sigma \approx 0.31$ at inner core densities, a typical value for solids and much lower than that of the inner core (0.44). This comparison suggests

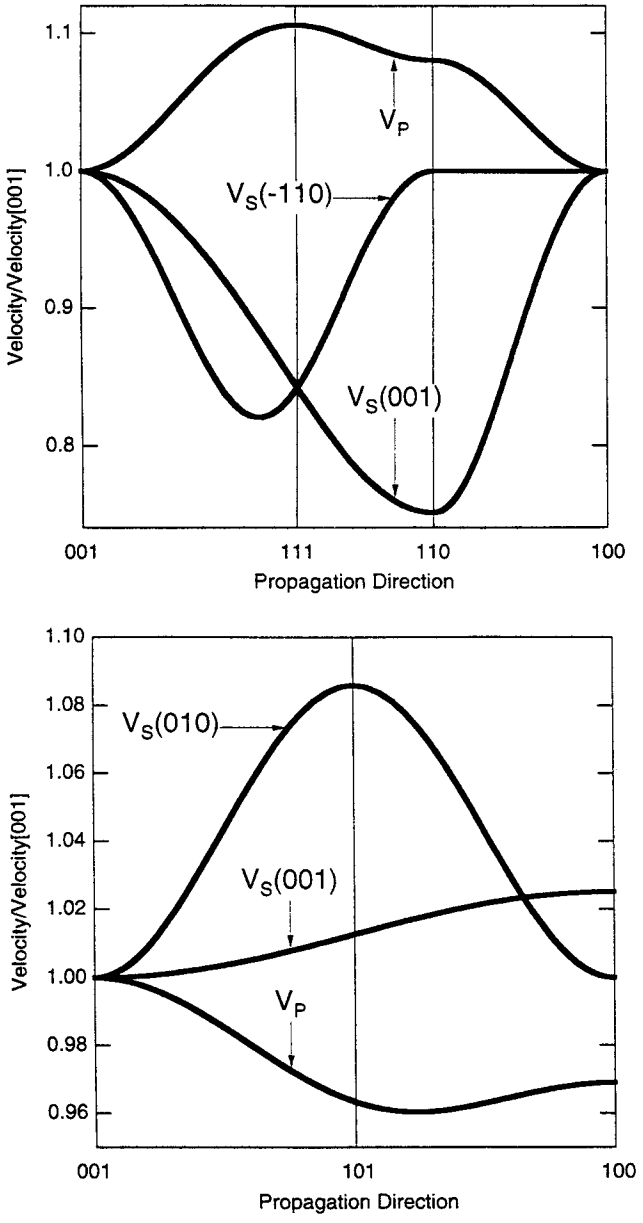

Figure 9. Velocity anisotropy in fcc (top) and hcp (bottom) iron at the density of the inner core (V=48 Bohr^3). Velocities are normalized to those for propagation in the [001] direction. Planes of polarization of S-waves are indicated. From *Stixrude and Cohen* [1995a].

that the anomalously high σ of the inner core may be due to anelasticity and dispersion at high temperature [*Jackson*, 1994].

High Temperature Properties

Our calculations of the static equation of state of iron show that the largest part of the pressure in the core is athermal - the static pressure of hcp iron at the density of the inner core is 240 GPa, more than 65% of the pressure at Earth's center. However, the thermal contribution to the pressure is non-negligible. In a metal, such as iron, there are two important contributions: (1) The pressure due to the thermal excitation of electrons. This term is unique to metals and arises from the population of high energy electronic states according to the Fermi-Dirac distribution. (2) The thermal pressure due to atomic vibrations. This contribution is also present in insulators.

At inner core densities, we find that the pressure due to the thermal excitation of electrons is approximately 10 GPa. The pressure due to atomic vibrations contributes approximately 50 GPa to the total pressure at inner core densities or 15% of the total pressure. The three contributions to the total pressure are shown separately along the T=6000 K isotherm in Figure 10. By combining LAPW calculations of the static pressure and that due to the thermal excitation of electrons, with cell model determinations of the thermal pressure, we obtain a complete description of the equation of state of iron.

Our theoretical high temperature equation of state of iron is in good agreement with available experimental data [*Wasserman et al.*, 1996]. We have shown that the Hugoniot calculated with the cell model and our tight binding Hamiltonian is within a few GPa of the experimental Hugoniot at core pressure. Our predicted Hugoniot temperatures are in excellent agreement with the estimates of *Brown and McQueen* [1986], but fall approximately 800 K lower than the values measured by *Yoo et al.* [1993]. We have also compared our equation

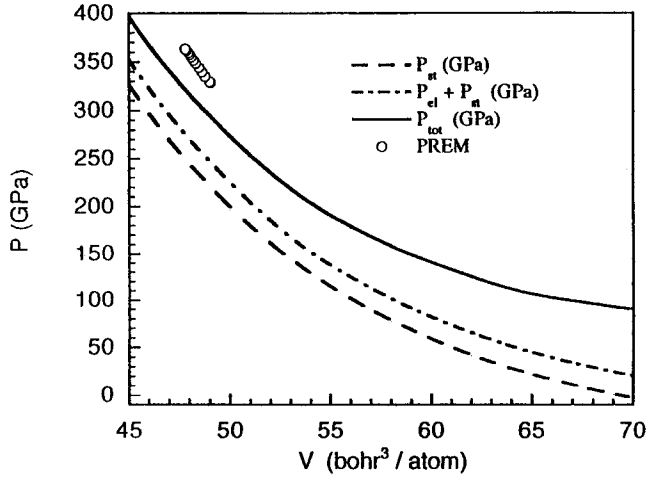

Figure 10. Different contributions to pressure at T=6000 K: static pressure (dashed line), static +electronic pressure (dot-dashed line), total pressure (solid line). Also shown is the pressure in the inner core according to PREM model (circles).

of state to measurements of the thermal expansivity of hcp and fcc iron and found good agreement.

We compare our equation of state of iron to the properties of the inner core as determined seismologically (Fig. 11). For temperatures in the middle of the range typically estimated for the inner core (6000 K) the density of iron is 3.5% greater than that of the inner core. This difference is larger than the estimated uncertainty in our theoretical equation of state - the difference between our results and comparable experimental data (e.g., the Hugoniot) is substantially less (1%). The difference between the density of iron and of the inner core also lies outside uncertainties in the seismological estimates of the inner core density. [*Masters and Shearer*, 1990]. We note that even for temperatures as high as 8000 K, somewhat higher than the highest estimates of inner core temperatures, iron is still 1% denser than the inner core.

We find that temperatures in excess of 8000 K are required for the density of iron to coincide with that of the inner core. The conclusion that very high temperatures are necessary is consistent with previous results, although the requisite temperatures found here are somewhat higher than those found by *Jephcoat and Olson* [1987]. These authors found that a temperature of 7000 K was adequate to yield agreement between the equation of state of iron and the inner core. The differences between our result and theirs is due to the different equations of state used. Because of the limited experimental data then available, Jephcoat and Olson were forced to extrapolate their semiempirical equation of state well outside the range of measurements. They also did not include an explicit division of vibrational and electronic thermal pressures.

DISCUSSION AND CONCLUSIONS

It is now possible to understand the physics of iron at the pressures and temperatures of the Earth's core on the basis of density functional theory. LAPW calculations, and parametric extensions of first principles methods, such as our tight binding method, allow one to predict, independently of experimental data, the physical behavior of iron at extreme conditions. Together with experimental measurement, these results place new constraints on the composition of the core, its thermal state, the crystalline structure of the inner core, and the origin of its anisotropy.

Density functional theory places some of the first constraints on the crystalline structure of the inner core. All of the observed structures of iron have been considered as the stable phase at inner core conditions [*Anderson*, 1986; *Ross et al.*, 1990; *Jeanloz* 1990]. Density functional theory effectively eliminates one of these phases, bcc, as a likely constituent of the inner core. We find that it is highly unfavorable energetically with respect to hcp and fcc phases at high pressure, primarily because of its larger volume. More importantly, we find that it is mechanically unstable - it violates the Born stability criterion above 150 GPa.

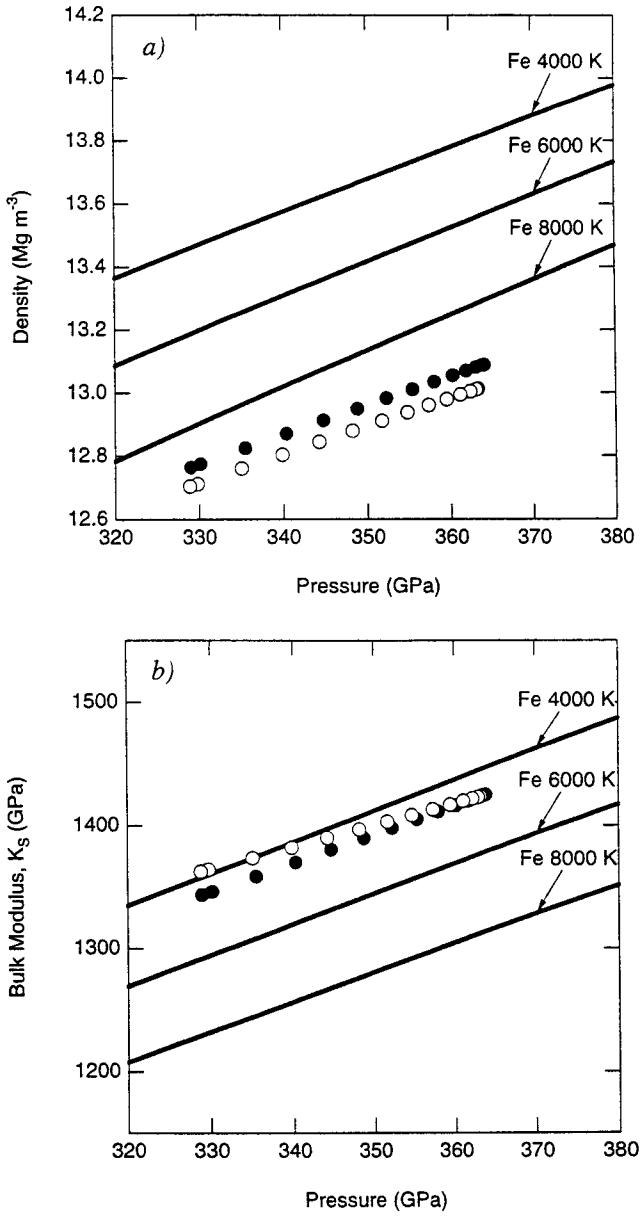

Figure 11. Density of pure iron along three isotherms (solid lines) compared with that of the inner core. The properties of the inner core are represented by the seismological models of *Dziewonski and Anderson* [1981] (solid circles) and *Dziewonski et al.* [1975] (open circles).

Our calculations favor a hexagonal phase as the crystalline structure of the inner core. We find that hcp is the stable low temperature phase from 11 GPa, to pressures well beyond those of the inner core. Moreover, we find that the elastic anisotropy of the hcp phase provides a natural explanation of the anisotropy of the inner core. We find that the P-wave anisotropy of hcp iron is very similar to that of the bulk inner core. Assuming that the inner core is a polycrystalline aggregate, we have shown that very simple textural models, combined with our predicted elastic constants, can account for seismic travel time observations. An aggregate in which the c-axes of the constituent hcp crystals are nearly aligned with the spin axis can account for 60% of the variance in BC-DF travel time anomalies. An alternative model, one which accounts for the seismic data equally well and is motivated by the strong alingment that is required, is that the inner core consists of a single crystal of hcp iron [*Stixrude and Cohen*, 1995a]. Based on these results, we cannot rule out the possibility that the inner core is composed of a different hexagonal phase (e.g., dhcp) which may be similar to hcp elastically and energetically.

First principles calculations show that the magnetic state of iron at high pressures is likely to be very different from its familiar low pressure state. The hcp and fcc phases are expected to be nonmagnetic at high pressure. This means that not only is the net magnetic moment zero, but that magnetic moments do not exist, even locally: spin pairing is complete. This is to be contrasted with the state of iron at zero pressure, where, above its Curie temperature, the net magnetic moment may be zero, but local moments, while disordered, remain virtually undiminished in magnitude from their values in the ferromagnetic, low-temperature state.

Our theoretical equation of state of iron at high pressures and temperatures shows that the Earth's inner core is not likely to be composed of pure iron. The alloying elements must be lighter on average than iron. The amount of the light element in the inner core remains uncertain, but is likely to be several weight %, depending on the identity of the light element (S, O, ...), and the as yet poorly constrained properties of the relevant alloys.

Acknowledgments. This work was supported by the National Science Foundation under grants EAR-9305060 (LPS) and EAR-9304624 (REC). Calculations were performed on the Cray C90 at the Pittsburgh Supercomputer Center, the IBM SP2 at the Cornell Theory Center, and the Cray J90 at the Geophysical Laboratory.

REFERENCES

Anderson, O. L., Properties of iron at the earth's core conditions, Geophys. *J. R. Astr. Soc., 84*, 561-579, 1986.

Asada, T., and K. Terakura, Cohesive properties of iron obtained by use of the generalized gradient approximation, *Phys. Rev. B, 46*, 13,599-13,602, 1992.

Bagno, P., O. Jepsen, and O. Gunnarson, Ground-state properties of third-row elements with nonlocal density functionals, *Phys. Rev. B, 40*, 1997-2000, 1989.

Birch, F., Elasticity and composition of the Earth's interior, *J. Geophys. Res.*, 57, 227-286, 1952.

Born, M., and K. Huang, *Dynamical Theory of Crystal Lattices*, pp. 140-149, Oxford University Press, Oxford, 1954.

Brandes, E. A. (ed.), *Smithells Metals Reference Book*, Butterworths, London, 1983.

Brown, J. M., and R. G. McQueen, Phase transitions, Grüneisen parameter, and elasticity for shocked iron between 77 GPa and 400 GPa, *J. Geophys. Res., 91*, 7485-7494, 1986.

Cohen, R. E., M. J. Mehl, and D. A. Papaconstantopoulos, Tight-binding total-energy method for transition and noble metals, *Phys. Rev. B, 50*, 14,694-14,697, 1994a.

Cohen, R. E., L. Stixrude, and D. A. Papaconstantopoulos, A new tight-binding model of iron, towards high temperature simulations of the earth's core, in *High Pressure Science and Technology-1993*, edited by S. C. Schmidt, J. W. Shaner, G. A. Samara, and M. Ross, pp. 891-894, American Institute of Physics, 1994b.

Cowley, E. R., J. Gross, Z. X. Gong, and G. K. Horton, Cell-cluster and self-consistent calculations for a model sodium chloride crystal, *Phys. Rev. B, 42*, 3135-3141, 1990.

Dziewonski, A. M., A. L. Hales, and E. R. Lapwood, Parametrically simple earth models consistent with geophysical data, *Phys. Earth Planet. Int., 10*, 12-48, 1975.

Dziewonski, A. M., and D. L. Anderson, Preliminary reference Earth model, *Phys. Earth Planet. Int., 25*, 297-356, 1981.

Glatzmaier, G. A., and P. H. Roberts, A three-dimensional convective dynamo solution with rotating and finitely conducting inner core and mantle, *Phys. Earth Planet. Int., 91*, 63-75, 1995.

Gunnarson, O., and B. I. Lundqvist, Exchange and correlation in atoms, molecules, and solids by the spin-density-functional formalism, *Phys. Rev. B, 13*, 4274-4298, 1976.

Hohenberg, P., and W. Kohn, Inhomogeneous electron gas, *Phys. Rev., 136*, B864-B871, 1964.

Hollerbach, R., and C. A. Jones, Influence of the earth's inner core on geomagnetic fluctuations and reversals, *Nature, 365*, 541-543, 1993.

Holt, A. C., W. G. Hoover, S. G. Gray, and D. R. Shortle, Comparison of the lattice-dynamics and cell-model approximations with Monte-Carlo thermodynamic properties, *Physica, 49*, 61-76, 1970.

Jackson, I., Viscoelastic relaxation in iron and the shear modulus of the inner core, in *High Pressure Science and Technology-1993*, edited by S. C. Schmidt, J. W. Shaner, G. A. Samara, and M. Ross, pp. 939-942, American Institute of Physics, 1994.

Jeanloz, R., The nature of the earth's core, *Ann. Rev. Earth Planet. Sci, 18*, 357-386, 1990.

Jeanloz, R. and H. R. Wenk, Convection and anisotropy of the inner core, *Geophys. Res. Lett., 15*, 72-75, 1988.

Jephcoat, A. P., H. K. Mao, and P. M. Bell, The static compression of iron to 78 GPa with rare gas solids as pressure transmitting media, *J. Geophys. Res., 91*, 4677-4684, 1986.

Jephcoat, A. P., and P. Olson, Is the inner core of the Earth pure iron, *Nature, 325*, 332-335, 1987.

Karato, S., Inner core anisotropy due to the magnetic field induced preferred orientation of iron, *Science, 262*, 1708-1711, 1993.

Kohn, W., and L. J. Sham, Self-consistent equations including exchange and correlation effects, *Phys. Rev., 140*, A1133-A1138, 1965.

Leung, T. C., C. T. Chen, and B. N. Harmon, Ground-state properties of Fe, Co, Ni, and their monoxides: results of the generalized gradient approximation, *Phys. Rev. B, 44*, 2923-2927, 1991.

Mao, H. K., Y. Wu, L. C. Chen, J. F. Shu, and A. P. Jephcoat, Static compression of iron to 300 GPa and $Fe_{0.8}Ni_{0.2}$ alloy to 260 GPa - implications for composition of the core, *J. Geophys. Res., 95*, 21,737-21,742, 1990.

Marcus, P. M., and V. L. Moruzzi, Stoner model of ferromagnetism and total-energy band theory, *Phys. Rev. B, 38*, 6949-6953, 1988.

Masters, T. G., and P. M. Shearer, Summary of seismological constraints on the structure of the Earth's core, *J. Geophys. Res., 95*, 21,691-21,695, 1990.

Mehl, M. J., J. E. Osburn, D. A. Papaconstantopoulos, and B. M. Klein, *Phys. Rev. B, 41*, 10,311, 1990.

McMahan, A. K. and M. Ross, High-temperature electron-band calculations, *Phys. Rev. B, 15*, 718-725, 1977.

Mermin, N. D., Thermal properties of the inhomogeneous electron gas, *Phys. Rev., 137*, A1441-A1444, 1965.

Morelli, A., A. M. Dziewonski, and J. H. Woodhouse, Anisotropy of the inner core inferred from PKIKP travel times, *Geophys. Res. Lett., 13*, 1545-1548, 1986.

Moroni, E. G., G. Grimvall, and T. Jarlborg, Free energy contributions to the hcp-bcc transformation in transition metals, *Phys. Rev. Lett., 76*, 2758-2761, 1996.

Perdew, J. P. and Y. Wang, Accurate and simple analytic representation of the electron-gas correlation energy, *Phys. Rev. B, 45*, 13,244-13,249, 1992.

Ree, F. H. and A. C. Holt, Thermodynamic properties of the alkali-halide crystals, *Phys. Rev. B, 8*, 826-842, 1973.

Ross, M., D. A. Young, and R. Grover, Theory of the iron phase diagram at Earth core conditions, *J. Geophys. Res., 95*, 21,713-21,716, 1990.

Sherman, D. M., Stability of possible Fe-FeS and Fe-FeO alloy phases at high pressure and the composition of the earth's core, *Earth Planet. Sci. Lett., 132*, 87-98, 1995.

Slater, J. C. and G. F. Koster, Simplified LCAO method for the periodic potential problem, *Phys. Rev., 94*, 1498-1524, 1954.

Söderlind, P., J. A. Moriarty, and J. M. Willis, First-principles theory of iron up to earth-core pressures: structural, vibrational, and elastic properties, *Phys. Rev. B, 53*, 14,063-14,072, 1996.

Song, X. D. and P. G. Richards, Seismological evidence for differential rotation of the earth's inner core, *Nature, 382*, 221-224, 1996.

Stixrude, L., R. E. Cohen, and D. J. Singh, Iron at high pressure: Linearized-augmented-plane-wave computations in the generalized-gradient approximation, *Phys. Rev. B*, 50, 6442-6445, 1994.

Stixrude, L., and R. E. Cohen, High pressure elasticity of iron and anisotropy of earth's inner core, *Science, 267*, 1972-1975, 1995a.

Stixrude, L., and R. E. Cohen, Constraints on the crystalline structure of the inner core - mechanical instability of bcc iron at high pressure, *Geophys. Res. Lett., 22*, 125-128, 1995b.

Tromp, J., Support for anisotropy of the earth's core from free oscillations, *Nature, 366*, 678-681, 1993.

Wallace, D. C., Thermodynamics of Crystals, John Wiley \& Sons, New York, 1972.

Wasserman, E., L. Stixrude, and R. E. Cohen, Thermal properties of iron at high pressures and temperatures, *Phys. Rev. B*, 53, 8296, 1996.

Wei, S., and H. Krakauer, Local-density-functional calculation of the pressure-induced metallization of BaSe and BaTe, *Phys. Rev. Lett., 55*, 1200, 1985.

Woodhouse, J. H., D. Giardini, and X. D. Li, Evidence for inner core anisotropy from free oscillations, *Geophys. Res. Lett., 13*, 1549-1552, 1986.

Yoo, C. S., N. C. Holmes, M. Ross, D. J. Webb, et al., Shock temperatures and melting of iron at earth core conditions, *Phys. Rev. Lett., 70*, 3931-3934, 1993.

R. E. Cohen, Geophysical Laboratory, 5251 Broad Branch Rd. NW, Washington, DC 20015-1305.

L. Stixrude, School of Earth and Atmospheric Sciences, Georgia Institute of Technology, Atlanta, GA 30332-0340.

E. Wasserman, 3200 Q Av. ETB-K9-77 Battelle, Pacific Northwest National Laboratory, Richland, WA 99352.

Geophysical Monograph Series

Including
IUGG Volumes
Maurice Ewing volumes
Mineral Physics Volumes